Can the Dielectric Constant of Fullerene Derivatives Be Enhanced by Side-Chain Manipulation? A Predictive First-Principles Computational Study

Sami, Selim; Haase, Pi A. B.; Alessandri, Riccardo; Broer, Ria; Havenith, Remco W. A.

Published in:
The Journal of Physical Chemistry. A: Molecules, Spectroscopy, Kinetics, Environment, & General Theory

DOI:
10.1021/acs.jpca.8b01348

Publication date:
2018

THE JOURNAL OF PHYSICAL CHEMISTRY A

Article

Cite This: J. Phys. Chem. A 2018, 122, 3919−3926

pubs.acs.org/JPCA

Can the Dielectric Constant of Fullerene Derivatives Be Enhanced by Side-Chain Manipulation? A Predictive First-Principles Computational Study

Published as part of The Journal of Physical Chemistry virtual special issue "Manuel Yáñez and Otilia Mó Festschrift".

Selim Sami,[†,‡] Pi A.B. Haase,[§] Riccardo Alessandri,[‡,∥] Ria Broer,[‡] and Remco W.A. Havenith*[,†,‡,⊥]

[†]Stratingh Institute for Chemistry, [‡]Zernike Institute for Advanced Materials, [§]Van Swinderen Institute, and [∥]Groningen Biomolecular Sciences and Biotechnology Institute, University of Groningen, Nijenborgh 4, 9747 AG Groningen, The Netherlands

[⊥]Department of Inorganic and Physical Chemistry, Ghent University, Krijgslaan 281−(S3), B-9000 Ghent, Belgium

Supporting Information

ABSTRACT: The low efficiency of organic photovoltaic (OPV) devices has often been attributed to the strong Coulombic interactions between the electron and hole, impeding the charge separation process. Recently, it has been argued that by increasing the dielectric constant of materials used in OPVs, this strong interaction could be screened. In this work, we report the application of periodic density functional theory together with the coupled perturbed Kohn−Sham method to calculate the electronic contribution to the dielectric constant for fullerene C_{60} derivatives, a ubiquitous class of molecules in the field of OPVs. The results show good agreement with experimental data when available and also reveal an important undesirable outcome when manipulating the side chain to maximize the static dielectric constant: in all cases, the electronic contribution to the dielectric constant decreases as the side chain increases in size. This information should encourage both theoreticians and experimentalists to further investigate the relevance of contributions to the dielectric constant from slower processes like vibrations and dipolar reorientations for facilitating the charge separation, because electronically, enlarging the side chain of conventional fullerene derivatives only lowers the dielectric constant, and consequently, their electronic dielectric constant is upper bound by the one of C_{60}.

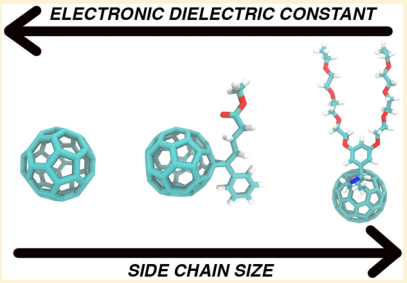

1. INTRODUCTION

Organic photovoltaic (OPV) devices, while currently lacking the high efficiencies of their inorganic counterparts, have key advantages that make them a promising candidate as an important renewable energy source for the future. The low manufacturing costs by using printing tools, suitability to be a triple green (manufacturing, energy production, recycling) energy source, flexibility, and low weight are among these advantages. Even though the efficiency of OPVs has increased from 2.5%[1] in 2001 to 13.1% in 2017,[2] these devices are still in need of a breakthrough to compete with silicon PV that is currently dominating commercially, with its efficiencies going over 26%.[3]

The lower efficiency of OPVs has been attributed to their excitonic nature:[4−6] absorption of light leads to strongly bound electron−hole pairs called excitons. To create a driving force toward charge separation in spite of this strong interaction, a commonly employed method is the use of a bulk heterojunction, which is comprised of domains of donor and acceptor materials. In such devices, excitons must diffuse to a donor−acceptor interface, where the charge separation can occur. The size of these donor and acceptor domains is an important consideration for such devices, since too large domains prevent the excitons to reach an interface due to their limited lifetime, whereas too small domains prevent the successful transport of separated charges to their respective electrodes.[7,8]

Instead of circumventing the problem of strongly bound excitons by the use of a bulk heterojunction, an alternative approach suggested by Koster et al.[9] is to search for high dielectric constant materials to solve it. The reasoning is that a higher dielectric constant would provide a higher screening of the Coulombic interactions between the charges and therewith effectively decrease the exciton binding energy and increase the exciton lifetime. Most solids consisting of organic molecules have low dielectric constants ($\varepsilon_r \approx 2-4$), compared to silicon ($\varepsilon_r = 12$).[10] Koster and co-workers have argued that increasing the dielectric constant would make solar cells with power conversion efficiencies of 20% feasible and that, with a large enough dielectric constant ($\varepsilon_r \approx 9$), the exciton binding energy would reduce to the thermal energy available at room temperature (k_bT). This would make bulk heterojunctions no longer necessary, since the absorption of photons would

Received: February 7, 2018
Revised: March 21, 2018
Published: March 21, 2018

DOI: 10.1021/acs.jpca.8b01348
J. Phys. Chem. A 2018, 122, 3919−3926

directly lead to the creation of free electrons and holes, essentially bridging the gap between organic and inorganic PVs.

The dielectric constant is a frequency-dependent property. A system can polarize in response to an electric field through different processes at different time scales. At high frequencies (femtosecond time scale), only electrons are able to respond to a rapidly oscillating electric field. This constitutes the electronic or optical dielectric constant (ϵ^{∞}). In the infrared region, small movements of nuclei (changing bond lengths, angles) can also relax the system in response to an electric field, giving the vibrational contribution to the dielectric constant. At a lower and wider range of frequencies, more elaborate nuclear movements can take place such as molecular reorientations and torsional rotations, contributing to the dipolar part of the dielectric constant. While large molecular reorientations often only occur in liquids and gases, some degree of torsional rotations can also occur in solids depending on the flexibility of these molecules. The overall (static) dielectric constant (ϵ^{0}) can then be obtained by combining these three contributions.

Experimental work has been done to increase the static dielectric constant of donor and acceptor materials that are commonly used in OPVs.[4,11−19] One recurring method is to introduce a flexible and polar ethylene glycol chain to fullerene derivatives, small molecules, and polymers. These studies have mostly been focused on maximizing the static dielectric constant. However, considering that silicon's high dielectric constant is fully electronic, it is surprising that the relevance of the static dielectric constant (i.e., atomic and dipolar contributions) to the field of OPVs is a topic not often discussed. We believe that more attention must be given to check whether these slower processes that involve nuclear motion are fast enough to facilitate the charge separation in solids. Furthermore, recent work by Torabi et al.[20,21] shows that experimental determination of dielectric constants in thin films can be susceptible to effects of doping and surface roughness, which can add a degree of uncertainty and unreliability to the obtained results. While a computational approach to calculate the dielectric constant is not without challenges, a successful method could provide the much-needed insight into how to systematically increase the dielectric constant to the point where the excitonic behavior of OPVs could be overcome. Moreover, it could also help distinguish between contributions to the dielectric constant that are relevant for OPVs.

Aside from the time scale discussion, the length scale relevance of the dielectric constant has also been questioned. The dielectric constant, being a bulk property, becomes relevant when two charges are separated by a medium large enough that the screening of electrostatic interactions becomes proportional to $1/\epsilon$. Van Duijnen et al.[22] have shown that a 1 nm separation is too small for this to occur. However, for OPVs, Bakulin et al.[23] have shown that, upon absorption of a photon, short-lived delocalized states help the initial separation of the hole and the electron. Therefore, Coulombic interactions become important at larger separations, where also the dielectric constant can be assumed to be relevant.

On the modeling side, Few et al.,[24] also interested in the applications to OPVs, used a coarse-grained theoretical model in which each fullerene derivative is treated as a single polarizable site, allowing to investigate large systems be it at a rather low theoretical detail and chemical specificity of the molecules. Heitzer et al.[25−28] used two-dimensional (2D) periodic density functional theory (DFT) to perform dielectric constant calculations on monolayers of substituted alkene chains, which are of interest for organic field effect transistors (OFETs), showing impressive dielectric constants up to 13 for these simple molecules. While these large values are quite encouraging, we briefly show in the theory section an inherent problem with calculation of the dielectric constant in 2D periodic systems that can easily result in large overestimations. Caleman et al.[29] performed molecular dynamics simulations on a large number of small organic molecules to calculate the vibrational and dipolar contribution to the dielectric constant using various force fields. Their work evidenced the problems of standard force fields in reproducing static dielectric constants even for simple organic molecules.

In this study, we focus on the calculation of the electronic dielectric constant (ϵ^{∞}). We use three-dimensional (3D) periodic DFT, as it allows a full quantum-mechanical treatment of the bulk system. After the geometry and the lattice parameters are optimized, the dielectric constant is obtained by the coupled perturbed Kohn−Sham method, which calculates the analytical second derivative of the energy with respect to an external electric field to obtain the polarizability.[30] The polarizability (α) is then related to the dielectric constant (ϵ) by eq 1 for bulk systems, where V is the volume of the unit cell:[30,31]

$$\epsilon = 1 + \frac{4\pi\alpha}{V} \tag{1}$$

For the calculation of ϵ^{∞}, fullerene C_{60} derivatives were chosen, as they are among the most commonly used acceptor materials due to their optical and electronic properties and relatively high electron mobility. Increasing the dielectric constant of these materials while retaining their optical properties can lead to more efficient solar cells. Fullerene derivatives used in this study are shown in Figure 1. Phenyl-C61-butyric acid methyl ester (PCBM) is a well-known and frequent choice for organic solar cells. Recently, Jahani et al.[14] synthesized the fulleropyrrolidines with one and two triethylene glycol (TEG) chains PTEG-1 and PTEG-2, respectively, and also the reference molecule PP without the TEG side chain. They have shown that PTEG-1 and PTEG-2 have increased dielectric constants with respect to the reference PP molecule. [6,6]-Phenyl-C61-butyric acid benzyl ester (PCBBz) and [6,6]-phenyl-C61-butyric acid 2-dimethylamino-5-nitrobenzyl ester (PCBDN) are two molecules investigated by De Gier et al.[32] While PCBBz has a methyl group replaced by a phenyl group compared to PCBM, PCBDN has also the electron-withdrawing NO_2 and electron-donating NH_2 groups in para position on the phenyl ring to create a large dipole moment. Two PCBM derivatives with added permanent dipole moments were also investigated: PCBSF[33] containing a sulfone group and PCBTE−OH[34] containing a TEG chain with a terminal OH group. Another strategy is to incorporate atoms with a high polarizability like bromine and iodine into the side chain. To investigate the effects of such atoms, calculations on PCBM-5Br and PCBM-3I were performed. Five bromine and three iodine atoms were chosen to retain similar molecular weights. These atoms were added to the phenyl ring as shown in Figure 1.

The size of the fullerene derivatives (∼100 atoms per molecule) limits the number of molecules in the unit cell, which allows a computationally feasible optimization of the atomic positions and lattice parameters, which is the most expensive step in our method. Therefore, we suggest to calculate the dielectric constant using only one molecule in the unit cell. To

DOI: 10.1021/acs.jpca.8b01348
J. Phys. Chem. A 2018, 122, 3919−3926

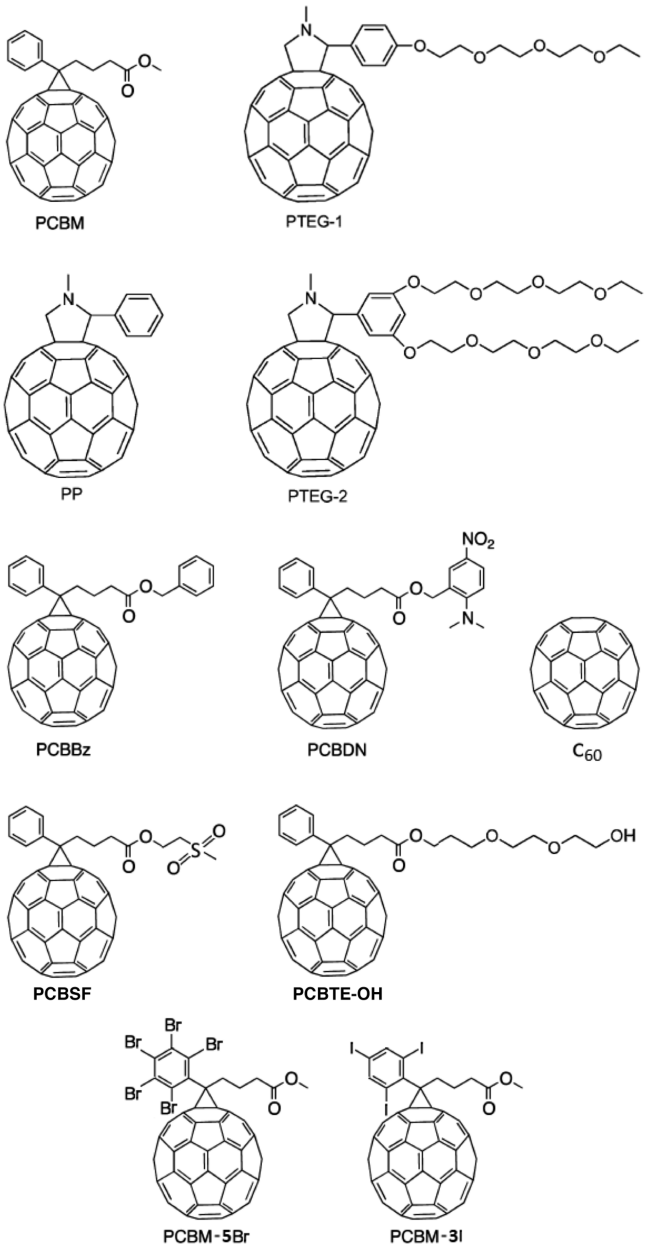

Figure 1. Fullerene derivatives studied in this work.

validate the use of a single molecule per unit cell, we performed calculations on the dielectric constant of ethylene carbonate, which is chosen for its size, using a different number of molecules per unit cell, which also yield different degrees of amorphousness. We shall show that the number of molecules per unit cell has a minor effect on the calculated dielectric constant and that the small variation in the dielectric constant is mostly due to different densities. Using this knowledge, we then proceed to calculate the dielectric constant of the previously introduced fullerene derivatives. We show that adding bulkier side chains only reduces the electronic dielectric constant of fullerene derivatives, and we discuss the implications.

2. THEORY

In the coupled perturbed method, the effect of an external static electric field (ε^0) is added perturbatively to the Hamiltonian. Expanding the total energy as a perturbative series of the electric field components t, u, and v gives eq 2, where μ, α, β are the dipole moment, polarizability, and hyperpolarizability tensors, respectively.

$$E_{\text{tot}} = E^0_{\text{tot}} - \sum_t \mu_t \varepsilon_t^0 - \frac{1}{2}\sum_{t,u} \alpha_{tu}\varepsilon_t^0\varepsilon_u^0 + \frac{1}{3!}\sum_{t,u,v} \beta_{tuv}\varepsilon_t^0\varepsilon_u^0\varepsilon_v^0 + \ldots \tag{2}$$

While higher orders can also be calculated, for the purpose of computing the dielectric constant, eq 2 is truncated at the second order. Furthermore, on the one hand, the dipole moment μ_t and thus the polarization P is ill-defined in a bulk sample and not used in the periodic directions. On the other hand, one can define the change in polarization ΔP as a macroscopic property, and many bulk properties (polarizability, piezoelectricity, ferroelectric polarization) can be calculated with respect to a perturbation.[35,36] For the coupled perturbed method, ΔP with respect to an electric field will result in the second derivative α_{tu}[30,31] as shown in eq 3

$$E^{tu}_{\text{tot}} = \alpha_{tu} = -2\sum_{\mu,\nu} D^t_{\mu\nu}\Omega^u_{\mu\nu} \tag{3}$$

where D^t is the first derivative of the unperturbed density matrix with respect to the tth component of the perturbation, and Ω^u is the uth component of the perturbation matrix. While Ω^u matrix elements can be obtained from the eigenvalues and eigenvectors of the unperturbed system at almost no computational cost, calculation of the derivative of the density matrix D^t is done with an iterative self-consistent procedure.

Polarizability is then linked to the dielectric constant as in eq 1 but this time as a tensor for an anisotropic system, where δ_{tu} is the Kronecker delta:

$$\epsilon^\infty_{tu} = \delta_{tu} + 4\pi\frac{\alpha_{tu}}{V} \tag{4}$$

As discussed above, the dielectric constant becomes relevant at large separations between the hole and electron, and at such separations, one could also look at the isotropic dielectric constant, instead of the anisotropic contributions:

$$\epsilon^\infty = \frac{\epsilon^\infty_{xx} + \epsilon^\infty_{yy} + \epsilon^\infty_{zz}}{3} \tag{5}$$

The electronic dielectric constant ϵ^∞ can also be calculated using the finite field method, that is, by applying an electric field.[37] To apply an electric field in periodic directions, a sawtooth potential is used. With this method, a supercell that is 3−4 times the size of the unit cell is necessary to guarantee the convergence of the response field, which makes the calculation significantly more expensive. At convergence, finite field method gives results that agree with the coupled perturbed method, albeit at a much higher cost. This makes coupled perturbed Kohn−Sham theory the preferred method, since it allows the investigation of much larger systems.

The dielectric constant can also be calculated in a 2D periodic system as was done by Heitzer et al.[25−28] for monolayers. In the nonperiodic direction, the equation relating the polarizability to the dielectric constant takes a different form due to the surface charges that are not present in a 3D periodic system:

$$\epsilon^{2D} = \frac{1}{1 - 4\pi\frac{\alpha}{V}} \tag{6}$$

DOI: 10.1021/acs.jpca.8b01348
J. Phys. Chem. A 2018, 122, 3919−3926

Using this method, Heitzer et al. found substituted alkenes with dielectric constants up to 13.[27] The main difference between eq 6 and eq 1 is that, at higher dielectric constants, the denominator in eq 6 approaches zero, making the equation very sensitive to changes in polarizability and volume. This sensitivity is then coupled to the need to decide on the length of the molecule in the nonperiodic direction, and consequently the volume, since the length in the nonperiodic direction is not straightforward to define. For their monolayers, Heitzer et al. have chosen this length to be the distance between the terminal nuclei of the alkenes, thereby neglecting the electron density beyond the terminal nuclei. Especially with large atoms such as iodine this is not an obvious choice. Using their definition of the length, Heitzer et al. have obtained dielectric constants between 5 and 13 for different substituted alkenes. However, by adding a van der Waals radius to each terminal atom while defining the length, all these substituted alkenes give dielectric constants between 3 and 4 (Supporting Information). This shows that attempting to maximize the dielectric constant using eq 6 can be perilous due to its sensitivity, especially at the high values that might be of interest in the field of organic electronics.

3. METHODS

Periodic quantum chemical calculations were performed with the CRYSTAL14[38] software using atom-centered Gaussian-type basis sets. While the ethylene carbonate calculations were done using DFT with the GGA functional PBE, for fullerene derivatives, the hybrid functional B3LYP was used. GGA functionals are known to overestimate the polarizability for large conjugated systems such as fullerenes, and the inclusion of some Hartree−Fock exchange is known to balance this problem.[39] All ethylene carbonate calculations were done with the 6-31G(d,p) basis set, and for fullerene derivatives, geometry and lattice parameter optimizations were done with 6-31G(d,p), and the subsequent cheaper and more basis-set-dependent polarizability calculations were done using the 6-311G(d,p) basis set. For iodine and bromine atoms only the 6-311G(d,p) basis set was used due to the unavailability of the smaller basis set. The effect of different basis sets on the optimized geometries was found to be negligible. For molecules containing heavy atoms (Br, I), relativistic effects on the polarizability were investigated to check whether the use of nonrelativistic methods is justified for the calculation of the dielectric constant, and we found that they have a negligible effect on the results (Supporting Information). All ϵ^{∞} calculations were done with the coupled perturbed Kohn−Sham method. Grimme's D2 dispersion correction[40] was used for geometry and lattice parameter optimizations. In DFT-D2 theory, every functional has a different factor that is commonly used to scale the dispersion energy. Because of the overbinding tendency of the D2 dispersion correction for large carbon systems such as C_{60} as seen from our results and also reported by Grimme et al.,[41] this scaling factor was altered to obtain experimental densities. A 4 × 4 × 4 k-point mesh was used in all calculations with fullerene derivatives.

Ethylene carbonate, due to its small size, was used to test the effect of the number of molecules per unit cell—going from a unit cell with a single molecule to 2, 8, and 36 molecules. The two-molecule unit cell refers to a crystal structure,[42] where the two molecules are pointing in the opposite directions from each other as seen in Figure 2b. The other unit cells were obtained by molecular dynamics (MD) simulations following the scheme introduced at the end of this section. In the case of 1 molecule per unit cell, all molecules point in the same direction (Figure 2a). The unit cells with 8 and 36 molecules allow more random orientations to represent a more amorphous system as seen in Figure 2c,d. The MD and crystal structure geometries and lattice parameters were taken as an initial structure for further optimization with quantum mechanical (QM) methods in the cases of 1, 2, and 8 molecules per unit cell. The unit cell with 36 molecules was not further optimized with QM methods due to the high computational cost of the optimization. More information on the computational details for ethylene carbonate and the dependence of ϵ^{∞} on using different DFT functionals or the Hartree−Fock method can be found in the Supporting Information.

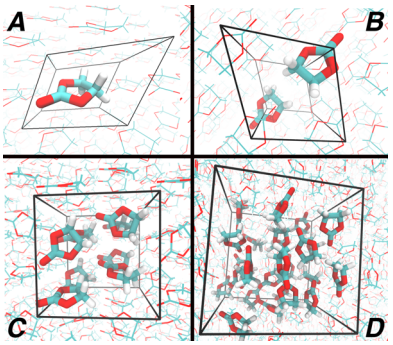

Figure 2. Unit cells of ethylene carbonate containing 1 (a), 2 (b), 8 (c), and 36 (d) molecules. Molecules from the neighboring unit cells are shown with thinner lines.

After the computational methods with ethylene carbonate were established, a similar approach was followed for the fullerene derivatives shown in Figure 1. From these molecules, only PCBM[43] and C_{60}[44] have known crystal structures (Figure 3), which were optimized in QM. For the rest, as the sizes of these molecules are quite large, calculations were performed using unit cells containing only a single fullerene molecule obtained by MD and later optimized by QM methods. It must be emphasized that the aim of such an approach is not to (re)produce experimental crystal structures, but instead, to obtain structures with reasonable molecular packing that can be used to calculate the dielectric constant. This approach is justified by the fact that our results do not significantly depend on the choice of the unit cell, not only for ethylene carbonate (Section 4.1) but also for PCBM (Section 4.3), where we find matching results from the experimental crystal structure and the one molecule unit cell calculations.

Except when crystal structures were available, initial geometries for unit cells were obtained from MD simulations using the software GROMACS 5.0.7.[45] Molecules were placed in a large unit cell and at a large separation from each other. The system was then compressed with a high-pressure NPT simulation, allowing the molecules to form a favorable morphology, followed by a relaxation at 1 atm. Topologies for these simulations were obtained from the automated topology builder (ATB)[46] for GROMOS 53A6 force field.[47] Since these geometries are subsequently quantum mechanically optimized, the quality of the automatically created topology was sufficient for this purpose.

4. RESULTS AND DISCUSSION

4.1. Ethylene Carbonate. Having a unit cell with multiple molecules allows multiple mutual orientations in a way to

DOI: 10.1021/acs.jpca.8b01348
J. Phys. Chem. A 2018, 122, 3919−3926

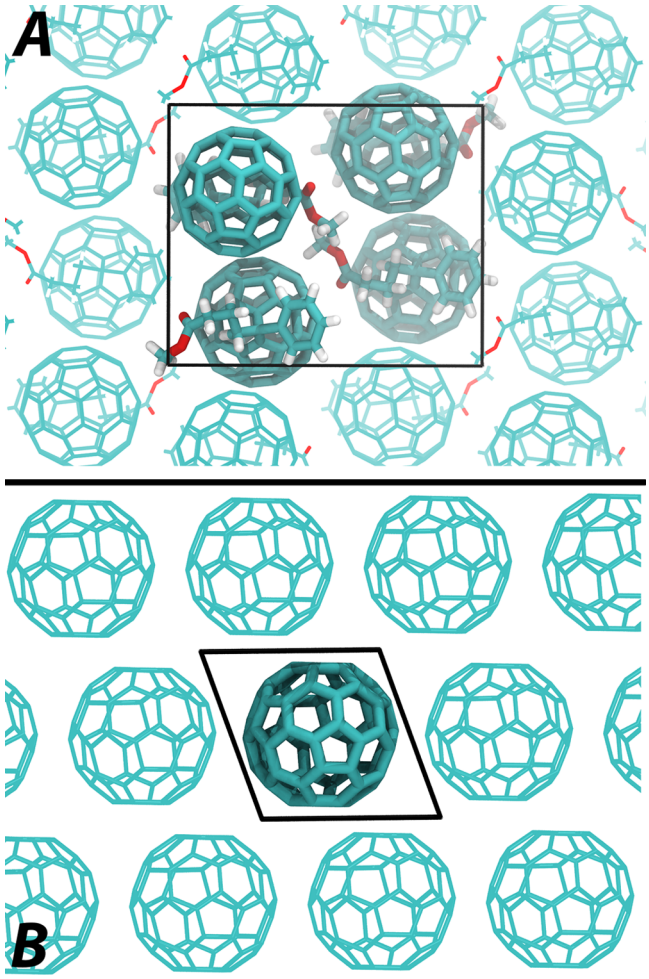

Figure 3. PCBM (a) and C_{60} (b) crystal structures used in this work.

represent an amorphous system. When the number of molecules is decreased, the system is forced to resemble more and more a crystalline structure. First, consequences for the dielectric constant of going from an amorphous system to a crystalline one are investigated. The electronic contribution (ϵ^{∞}) is ~2 for all different box sizes (Table 1). From these

Table 1. Density ρ (g/cm^3) and Dielectric Constant with Different Number of Molecules Per Unit Cell (#)

#	ρ (g/cm^3)	ϵ^{∞}
36	1.417	1.97
8	1.483	2.06
2	1.537	2.11
1	1.320	1.90

results, we conclude that whether it is an amorphous system or a crystalline one or whether it is a crystal with all dipoles pointing in the same direction (#1) or being canceled out by each other (#2), the isotropic ϵ^{∞} seems to be mostly unaffected. This observation encourages and justifies the use of small unit cells to reduce the computational costs when working with fullerene derivatives.

Observing that all systems give comparable results for ϵ^{∞}, the effect of density can be investigated by comparing the calculations performed with the same basis set and functional. As seen from eq 1, ϵ^{∞} is related to the volume and consequently to the density. Figure 4 shows that ϵ^{∞} is linearly correlated with the density for a given molecule: A higher

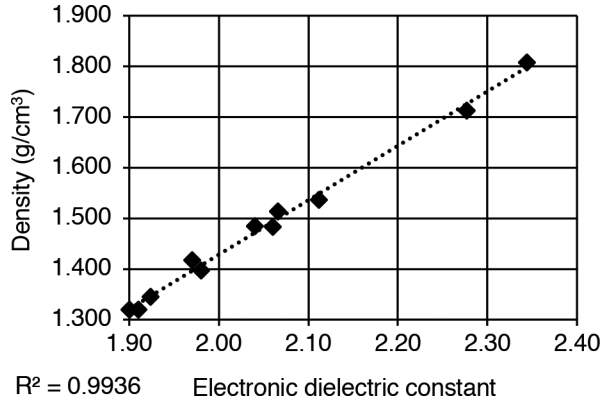

Figure 4. ϵ^{∞} vs density plot obtained from various calculations on ethylene carbonate performed with the same functional/basis set. Different densities obtained by both different number of molecules per unit cell and by optimizing the lattice parameters with different scaling factors for the dispersion correction (More information about the data points in the Supporting Information).

density leads to larger ϵ^{∞}. This knowledge suggests that higher packing and crystallinity are ideal for maximizing the electronic dielectric constant.

4.2. Obtaining Accurate Densities for Fullerene Derivatives. After the methods to be used in this work were validated, more complicated systems, namely, the fullerene derivatives, were investigated. Optimizing the lattice parameters for fullerene derivatives using the conventional DFT-D2 scaling factor for B3LYP (1.05) led to extremely high densities (~1.75 g/cm^3). This is consistent with what was previously observed for large carbon systems such as C_{60}.[41] Therefore, the scaling factor was adjusted to reproduce the experimental crystal structures for PCBM and C_{60} (Table 2), which are the only two

Table 2. Crystal Densities (g/cm^3) with Scaled Dispersion Correction Factor (f) and the Experimental Densities

	f: 1.05	f: 0.60	expt
PCBM crystal	1.774	1.646	1.620[43]
C_{60} crystal	1.754	1.644	1.649[44]

molecules in this study with known crystal structures and densities. A scaling factor of 0.60 was found to give densities that are in good agreement with the experimental densities, and thus this scaling factor was used in the subsequent calculations on the fullerene derivatives. More detailed information on how the density depends on the scaling factor can be found in the Supporting Information.

4.3. Dielectric Constant of Fullerene Derivatives. The dielectric constants of various fullerene derivatives were calculated using the methods outlined above. Results are shown in Table 3. The good agreement between the results of the one molecule unit cell calculation and the crystal structure of PCBM further corroborates the suitability of using small unit cells. From all the molecules studied, C_{60} has the highest ϵ^{∞}. This confirms that the high polarizability of fullerene derivatives is governed by the polarizable nature of the delocalized π electrons of the C_{60} moiety. Furthermore, as shown in Figure 5, there is a clear trend between the size and ϵ^{∞} of the fullerene

DOI: 10.1021/acs.jpca.8b01348
J. Phys. Chem. A 2018, 122, 3919−3926

Table 3. Dielectric Constants of Fullerene Derivatives

	ρ^a	ϵ^∞(calc)^b	ϵ^0(exp)^c	$\epsilon^0 - \epsilon^\infty$ ^{d}
C_{60}	1.644	3.83	3.61,[48] 4.08,[49] 4.4 ± 0.2[50]	−0.22, 0.25, 0.57 ± 0.2
PP	1.598	3.66	3.6 ± 0.4[14]	−0.06 ± 0.4
PCBM Crystal	1.646	3.57	3.9 ± 0.1[14]	0.33 ± 0.1
PCBM	1.645	3.57	3.9 ± 0.1[14]	0.33 ± 0.1
PCBBz	1.569	3.37		
PCBSF	1.551	3.21	3.9 ± 0.1[33]	0.69 ± 0.1
PCBDN	1.496	3.13	3.9 ± 0.2[34]	0.77 ± 0.2
PCBTE−OH	1.529	3.22	5.0 ± 0.1[33]	1.78 ± 0.1
PTEG-1	1.545	3.31	5.7 ± 0.2[14]	2.39 ± 0.2
PTEG-2	1.435	2.95	5.3 ± 0.2[14]	2.35 ± 0.2
PCBM-5Br	1.790	3.00		
PCBM-3I	1.935	3.29		

^{a}Density (g/cm^3). ^{b}Electronic contributions (ϵ^∞) are calculated. ^{c}Static dielectric constants (ϵ^0) are experimental values. ^{d}The final column is the difference between the two previous columns, which can be used to approximate the vibrational and dipolar contributions.

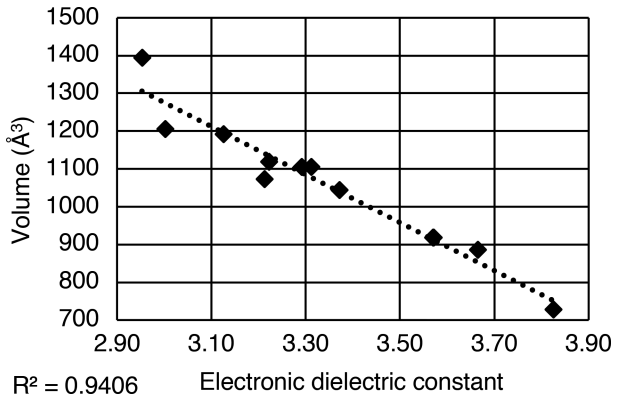

Figure 5. ϵ^∞ vs the unit cell volume for the fullerene derivatives in Table 3.

derivatives: The larger the side chain, the lower ϵ^∞ will be. Here the dielectric constant is plotted against the volume of the unit cell. Considering that the C_{60} occupies the same volume in each case, the change in the unit cell volume can be fully attributed to the side chain.

A similar trend is also seen for the density in Figure 6. C_{60} has the highest density among the molecules that do not contain heavy atoms (Br, I), and as the density decreases, ϵ^∞ also decreases. The density decreases for fullerene derivatives due to the mixing of high-density C_{60} with lower-density side

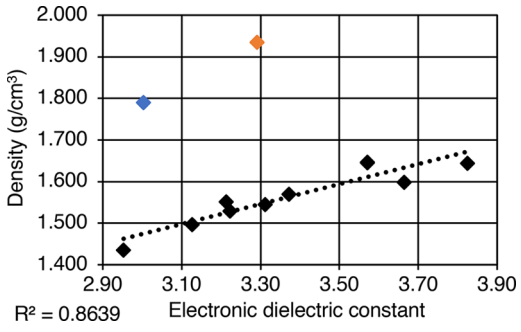

Figure 6. ϵ^∞ vs density of the system for molecules in Table 3. R^2 is calculated without PCBM-3I (orange diamond) and PCBM-5Br (blue diamond).

chains and also because the packing becomes worse compared to a C_{60} crystal structure. In the case of PCBM-5Br and PCBM-3I, densities much higher than the one of C_{60} are observed, while their ϵ^∞ is comparable to the rest of the molecules. This is because even though heavy atoms contribute a lot to increasing the density, their electron density is mostly due to core electrons, which have a minimal effect on the polarizability. When the side chain size is plotted against ϵ^∞ (Figure 5), these molecules also fit with the other fullerene derivatives. This shows that no special behavior is observed by adding heavy atoms such as iodine or bromine to fullerene derivatives.

Experimental measurement of ϵ^∞ by ellipsometry for the PCBM molecule was done by Guilbert et al.[51] Their result of 3.4 is in good agreement with our obtained value of 3.57. For C_{60}, there are two ellipsometry measurements with somewhat different values (3.6,[48] 4.08[49]), and our calculated ϵ^∞ lies between these two measurements (3.83). Another experimental value of 4.4 ± 0.2 for C_{60} has been obtained[50] by capacitance measurements. This value is higher than the ones from ellipsometry measurements. Ren et al.[49] argue that this difference is due to the inclusion of the contributions from phonon absorption in the infrared region with the capacitance measurements.

Finally, we focus on the difference between the calculated ϵ^∞ and the experimental ϵ^0 values when available. ϵ^0 measurements were done at low frequency, so that on top of the electronic contribution, one would also expect vibrational and dipolar contributions to the dielectric constant. Therefore, the difference column in Table 3 would be a good approximation for the vibrational and/or dipolar contribution to the dielectric constant. It can be seen that, for PP, which has the smallest side chains, the difference is within the error margin, showing that there is no or a very small vibrational/dipolar contribution. If we compare PCBM with PCBDN or PCBSF, both possessing dipolar functional groups, we see that the difference increases from 0.33 to 0.77 and 0.69, respectively. However, most intriguingly, for molecules containing the highly flexible TEG chain (PTEG-1, PTEG-2, PCBTE−OH), there is a large difference between ϵ^∞ and ϵ^0 (~2). It could be argued that, while for the other molecules only vibrational motion contributes to the dielectric constant, for TEG-containing molecules, due to their flexibility, larger-scale dipolar reorientations give an increased contribution to the static dielectric constant. The difference between ϵ^∞ and ϵ^0 was also shown experimentally for TEG-containing small molecules,[13] where ϵ^0 decreases from 8 to 10 to 3−4 at high frequencies. This dipolar contribution can also be computed using molecular dynamics simulations and is the subject of further studies.

5. CONCLUSIONS

Using 3D periodic DFT calculations, the electronic dielectric constant (ϵ^∞) of fullerene derivatives was calculated. It was shown that ϵ^∞ decreases as the side chain size increases. Furthermore, the difference between theoretical ϵ^∞ and the experimental static dielectric constant (ϵ^0), which can be considered to be mostly the vibrational/dipolar contribution to the dielectric constant, increases when flexible molecules containing TEG chains are used. From these observations, it could be argued that, to get a high static dielectric constant, side chains should as much as possible be constituted by groups that contribute to the vibrational/dipolar part, so that any sacrifice in ϵ^∞ due to the "dilution" of C_{60} is compensated by an

DOI: 10.1021/acs.jpca.8b01348
J. Phys. Chem. A 2018, 122, 3919−3926

increase of vibrational/dipolar contribution to ϵ^0. However, such an approach would only be successful under the assumption that the vibrational/dipolar contributions occur at a time scale that is relevant for the working principles of OPVs. If that is not the case, then smaller side chains would be the ideal choice to maximize the electronic dielectric constant, which would also mean that the relevant part of the dielectric constant of conventional fullerene derivatives are upper bound by the one of C_{60}.

For prospective work, vibrational/dipolar contributions to the dielectric constant for fullerene derivatives will be calculated by molecular dynamics simulations to get an insight into the time scale of these contributions and to look for ways for "speeding up" these processes to a time scale more beneficial for facilitating the charge separation.

■ ASSOCIATED CONTENT

Supporting Information

The Supporting Information is available free of charge on the ACS Publications website at DOI: 10.1021/acs.jpca.8b01348.

Ethylene carbonate computational details, the effect of different functionals and Hartree−Fock method on the results, relativistic effects for heavy-atom-containing fragments, sensitivity of the dielectric constant to the chosen length of the molecule for 2D periodic calculations, density with different dispersion correction scaling factors, sample input for the dielectric constant calculation in CRYSTAL (PDF)

■ AUTHOR INFORMATION

Corresponding Author

*E-mail: r.w.a.havenith@rug.nl.

ORCID

Selim Sami: 0000-0002-4484-0322

Remco W.A. Havenith: 0000-0003-0038-6030

Notes

The authors declare no competing financial interest.

■ ACKNOWLEDGMENTS

We thank A. Borschevsky (Univ. of Groningen) for her contributions to the relativistic work, the Next Generation OPV Foundation of Fundamental Research on Matter (FOM) Focus Group, J. C. Hummelen (Univ. of Groningen) for fruitful discussions, and the Univ. of Groningen for the access to the Peregrine Computing Cluster. R.A. thanks The Netherlands Organisation for Scientific Research (NWO; Graduate Programme Advanced Materials, No. 022.005.006) for financial support. This work is part of the research programme of the FOM, which is part of NWO. This is a publication of the FOM Focus Group "Next Generation Organic Photovoltaics", participating in the Dutch Institute for Fundamental Energy Research.

■ REFERENCES

(1) Shaheen, S. E.; Brabec, C. J.; Sariciftci, N. S.; Padinger, F.; Fromherz, T.; Hummelen, J. C. 2.5% Efficient Organic Plastic Solar Cells. *Appl. Phys. Lett.* **2001**, *78*, 841−843.

(2) Zhao, W. C.; Li, S. S.; Yao, H. F.; Zhang, S. Q.; Zhang, Y.; Yang, B.; Hou, J. H. Molecular Optimization Enables over 13% Efficiency in Organic Solar Cells. *J. Am. Chem. Soc.* **2017**, *139*, 7148−7151.

(3) Yoshikawa, K. Silicon Heterojunction Solar Cell with Interdigitated Back Contacts for a Photoconversion Efficiency over 26%. *Nat. Energy* **2017**, *2*, 17032.

(4) Brebels, J.; Manca, J. V.; Lutsen, L.; Vanderzande, D.; Maes, W. High Dielectric Constant Conjugated Materials for Organic Photovoltaics. *J. Mater. Chem. A* **2017**, *5*, 24037−24050.

(5) Clarke, T. M.; Durrant, J. R. Charge Photogeneration in Organic Solar Cells. *Chem. Rev.* **2010**, *110*, 6736−6767.

(6) Gelinas, S.; Pare-Labrosse, O.; Brosseau, C. N.; Albert-Seifried, S.; McNeill, C. R.; Kirov, K. R.; Howard, I. A.; Leonelli, R.; Friend, R. H.; Silva, C. The Binding Energy of Charge-Transfer Excitons Localized at Polymeric Semiconductor Heterojunctions. *J. Phys. Chem. C* **2011**, *115*, 7114−7119.

(7) Brabec, C. J.; Heeney, M.; McCulloch, I.; Nelson, J. Influence of Blend Microstructure on Bulk Heterojunction Organic Photovoltaic Performance. *Chem. Soc. Rev.* **2011**, *40*, 1185−1199.

(8) Hedley, G. J.; Ruseckas, A.; Samuel, I. D. W. Light Harvesting for Organic Photovoltaics. *Chem. Rev.* **2017**, *117*, 796−837.

(9) Koster, L. J. A.; Shaheen, S. E.; Hummelen, J. C. Pathways to a New Efficiency Regime for Organic Solar Cells. *Adv. Energy Mater.* **2012**, *2*, 1246−1253.

(10) Dunlap, W. C.; Watters, R. L. Direct Measurement of the Dielectric Constants of Silicon and Germanium. *Phys. Rev.* **1953**, *92*, 1396−1397.

(11) Armin, A.; Stoltzfus, D. M.; Donaghey, J. E.; Clulow, A. J.; Nagiri, R. C. R.; Burn, P. L.; Gentle, I. R.; Meredith, P. Engineering Dielectric Constants in Organic Semiconductors. *J. Mater. Chem. C* **2017**, *5*, 3736−3747.

(12) Chen, X. X.; Zhang, Z. J.; Ding, Z. C.; Liu, J.; Wang, L. X. Diketopyrrolopyrrole-Based Conjugated Polymers Bearing Branched Oligo(Ethylene Glycol) Side Chains for Photovoltaic Devices. *Angew. Chem., Int. Ed.* **2016**, *55*, 10376−10380.

(13) Donaghey, J. E.; Armin, A.; Burn, P. L.; Meredith, P. Dielectric Constant Enhancement of Non-Fullerene Acceptors Via Side-Chain Modification. *Chem. Commun.* **2015**, *51*, 14115−14118.

(14) Jahani, F.; Torabi, S.; Chiechi, R. C.; Koster, L. J. A.; Hummelen, J. C. Fullerene Derivatives with Increased Dielectric Constants. *Chem. Commun.* **2014**, *50*, 10645−10647.

(15) Lu, Y. Z.; Xiao, Z. G.; Yuan, Y. B.; Wu, H. M.; An, Z. W.; Hou, Y. B.; Gao, C.; Huang, J. S. Fluorine Substituted Thiophene-Quinoxaline Copolymer to Reduce the HOMO Level and Increase the Dielectric Constant for High Open-Circuit Voltage Organic Solar Cells. *J. Mater. Chem. C* **2013**, *1*, 630−637.

(16) Torabi, S.; et al. Strategy for Enhancing the Dielectric Constant of Organic Semiconductors without Sacrificing Charge Carrier Mobility and Solubility. *Adv. Funct. Mater.* **2015**, *25*, 150−157.

(17) Zhang, S.; Zhang, Z. J.; Liu, J.; Wang, L. X. Fullerene Adducts Bearing Cyano Moiety for Both High Dielectric Constant and Good Active Layer Morphology of Organic Photovoltaics. *Adv. Funct. Mater.* **2016**, *26*, 6107−6113.

(18) Liu, X.; et al. A High Dielectric Constant Non-Fullerene Acceptor for Efficient Bulk-Heterojunction Organic Solar Cells. *J. Mater. Chem. A* **2018**, *6*, 395−403.

(19) Brebels, J.; Douvogianni, E.; Devisscher, D.; Eachambadi, R. T.; Manca, J.; Lutsen, L.; Vanderzande, D.; Hummelen, J. C.; Maes, W. An Effective Strategy to Enhance the Dielectric Constant of Organic Semiconductors - CPDTTPD-Based Low Bandgap Polymers Bearing Oligo(Ethylene Glycol) Side Chains. *J. Mater. Chem. C* **2018**, *6*, 500−511.

(20) Torabi, S.; Cherry, M.; Duijnstee, E. A.; Le Corre, V. M.; Qiu, L.; Hummelen, J. C.; Palasantzas, G.; Koster, L. J. A. Rough Electrode Creates Excess Capacitance in Thin-Film Capacitors. *ACS Appl. Mater. Interfaces* **2017**, *9*, 27290−27297.

(21) Torabi, S.; Liu, J.; Gordiichuk, P.; Herrmann, A.; Qiu, L.; Jahani, F.; Hummelen, J. C.; Koster, L. J. A. Deposition of LiF onto Films of Fullerene Derivatives Leads to Bulk Doping. *ACS Appl. Mater. Interfaces* **2016**, *8*, 22623−22628.

DOI: 10.1021/acs.jpca.8b01348
J. Phys. Chem. A 2018, 122, 3919−3926

(22) van Duijnen, P. T.; de Gier, H. D.; Broer, R.; Havenith, R. W. A. The Behaviour of Charge Distributions in Dielectric Media. *Chem. Phys. Lett.* **2014**, *615*, 83−88.
(23) Bakulin, A. A.; Rao, A.; Pavelyev, V. G.; van Loosdrecht, P. H. M.; Pshenichnikov, M. S.; Niedzialek, D.; Cornil, J.; Beljonne, D.; Friend, R. H. The Role of Driving Energy and Delocalized States for Charge Separation in Organic Semiconductors. *Science* **2012**, *335*, 1340−1344.
(24) Few, S.; Chia, C.; Teo, D.; Kirkpatrick, J.; Nelson, J. The Impact of Chemical Structure and Molecular Packing on the Electronic Polarisation of Fullerene Arrays. *Phys. Chem. Chem. Phys.* **2017**, *19*, 18709−18720.
(25) Heitzer, H. M.; Marks, T. J.; Ratner, M. A. Computation of Dielectric Response in Molecular Solids for High Capacitance Organic Dielectrics. *Acc. Chem. Res.* **2016**, *49*, 1614−1623.
(26) Heitzer, H. M.; Marks, T. J.; Ratner, M. A. Molecular-Donor-Bridge-Acceptor Strategies for High-Capacitance Organic Dielectric Materials. *J. Am. Chem. Soc.* **2015**, *137*, 7189−7196.
(27) Heitzer, H. M.; Marks, T. J.; Ratner, M. A. Maximizing the Dielectric Response of Molecular Thin Films Via Quantum Chemical Design. *ACS Nano* **2014**, *8*, 12587−12600.
(28) Heitzer, H. M.; Marks, T. J.; Ratner, M. A. First-Principles Calculation of Dielectric Response in Molecule-Based Materials. *J. Am. Chem. Soc.* **2013**, *135*, 9753−9759.
(29) Caleman, C.; van Maaren, P. J.; Hong, M. Y.; Hub, J. S.; Costa, L. T.; van der Spoel, D. Force Field Benchmark of Organic Liquids: Density, Enthalpy of Vaporization, Heat Capacities, Surface Tension, Isothermal Compressibility, Volumetric Expansion Coefficient, and Dielectric Constant. *J. Chem. Theory Comput.* **2012**, *8*, 61−74.
(30) Ferrero, M.; Rerat, M.; Orlando, R.; Dovesi, R. The Calculation of Static Polarizabilities of 1−3D Periodic Compounds. The Implementation in the CRYSTAL Code. *J. Comput. Chem.* **2008**, *29*, 1450−1459.
(31) Ferrero, M.; Rerat, M.; Kirtman, B.; Dovesi, R. Calculation of First and Second Static Hyperpolarizabilities of One- to Three-Dimensional Periodic Compounds. Implementation in the CRYSTAL Code. *J. Chem. Phys.* **2008**, *129*, 244110.
(32) de Gier, H. D.; Jahani, F.; Broer, R.; Hummelen, J. C.; Havenith, R. W. A. Promising Strategy to Improve Charge Separation in Organic Photovoltaics: Installing Permanent Dipoles in PCBM Analogues. *J. Phys. Chem. A* **2016**, *120*, 4664−4671.
(33) Douvogianni, E. Enhancing the Dielectric Constant of Organic Materials. Ph.D. Thesis, University of Groningen: Groningen, The Netherlands, 2018.
(34) Bahnamiri, F. J. Synthetic Strategies for Modifying Dielectric Properties and the Electron Mobility of Fullerene Derivatives. Ph.D. Thesis, University of Groningen: Groningen, The Netherlands, 2016.
(35) Ortiz, G.; Martin, R. M. Macroscopic Polarization as a Geometric Quantum Phase - Many-Body Formulation. *Phys. Rev. B: Condens. Matter Mater. Phys.* **1994**, *49*, 14202−14210.
(36) Martin, R. M. Comment on Calculations of Electric Polarization in Crystals. *Phys. Rev. B* **1974**, *9*, 1998−1999.
(37) Darrigan, C.; Rerat, M.; Mallia, G.; Dovesi, R. Implementation of the Finite Field Perturbation Method in the Crystal Program for Calculating the Dielectric Constant of Periodic Systems. *J. Comput. Chem.* **2003**, *24*, 1305−1312.
(38) Dovesi, R.; et al. CRYSTAL14: A Program for the Ab Initio Investigation of Crystalline Solids. *Int. J. Quantum Chem.* **2014**, *114*, 1287−1317.
(39) Champagne, B.; Perpete, E. A.; Jacquemin, D.; van Gisbergen, S. J. A.; Baerends, E. J.; Soubra-Ghaoui, C.; Robins, K. A.; Kirtman, B. Assessment of Conventional Density Functional Schemes for Computing the Dipole Moment and (Hyper)Polarizabilities of Push-Pull Pi-Conjugated Systems. *J. Phys. Chem. A* **2000**, *104*, 4755−4763.
(40) Grimme, S. Semiempirical Hybrid Density Functional with Perturbative Second-Order Correlation. *J. Chem. Phys.* **2006**, *124*, 034108.
(41) Grimme, S.; Antony, J.; Ehrlich, S.; Krieg, H. A Consistent and Accurate Ab Initio Parametrization of Density Functional Dispersion Correction (DFT-D) for the 94 Elements H-Pu. *J. Chem. Phys.* **2010**, *132*, 154104.
(42) Brown, C. J. The Crystal Structure of Ethylene Carbonate. *Acta Crystallogr.* **1954**, *7*, 92−98.
(43) Casalegno, M.; Zanardi, S.; Frigerio, F.; Po, R.; Carbonera, C.; Marra, G.; Nicolini, T.; Raos, G.; Meille, S. V. Solvent-Free Phenyl-C61-Butyric Acid Methyl Ester (PCBM) from Clathrates: Insights for Organic Photovoltaics from Crystal Structures and Molecular Dynamics. *Chem. Commun.* **2013**, *49*, 4525−4527.
(44) Dorset, D. L.; Mccourt, M. P. Disorder and the Molecular Packing of C-60 Buckminsterfullerene - a Direct Electron-Crystallographic Analysis. *Acta Crystallogr., Sect. A: Found. Crystallogr.* **1994**, *50*, 344−351.
(45) Abraham, M. J.; Murtola, T.; Schulz, R.; Páll, S.; Smith, J. C.; Hess, B.; Lindahl, E. GROMACS: High Performance Molecular Simulations through Multi-Level Parallelism from Laptops to Supercomputers. *SoftwareX* **2015**, *1−2*, 19−25.
(46) Malde, A. K.; Zuo, L.; Breeze, M.; Stroet, M.; Poger, D.; Nair, P. C.; Oostenbrink, C.; Mark, A. E. An Automated Force Field Topology Builder (ATB) and Repository: Version 1.0. *J. Chem. Theory Comput.* **2011**, *7*, 4026−4037.
(47) Oostenbrink, C.; Villa, A.; Mark, A. E.; Van Gunsteren, W. F. A Biomolecular Force Field Based on the Free Enthalpy of Hydration and Solvation: The GROMOS Force-Field Parameter Sets 53A5 and 53A6. *J. Comput. Chem.* **2004**, *25*, 1656−1676.
(48) Eklund, P. C.; Rao, A. M.; Wang, Y.; Zhou, P.; Wang, K. A.; Holden, J. M.; Dresselhaus, M. S.; Dresselhaus, G. Optical-Properties of C-60-Based and C-70-Based Solid Films. *Thin Solid Films* **1995**, *257*, 211−232.
(49) Ren, S. L.; et al. Ellipsometric Determination of the Optical-Constants of C60 (Buckminsterfullerene) Films. *Appl. Phys. Lett.* **1991**, *59*, 2678−2680.
(50) Hebard, A. F.; Haddon, R. C.; Fleming, R. M.; Kortan, A. R. Deposition and Characterization of Fullerene Films. *Appl. Phys. Lett.* **1991**, *59*, 2109−2111.
(51) Guilbert, A. A. Y.; et al. Spectroscopic Evaluation of Mixing and Crystallinity of Fullerenes in Bulk Heterojunctions. *Adv. Funct. Mater.* **2014**, *24*, 6972−6980.

DOI: 10.1021/acs.jpca.8b01348
J. Phys. Chem. A 2018, 122, 3919−3926